MOBILE ROBOTS FOR HAZARDOUS ENVIRONMENTS – NEW TECHNOLOGY FOR MOBILITY

Andrew A. Goldenberg [a, b]
[a] Engineering Services Inc. (ESI)
Automation & Robotics Systems
890 Yonge Street, Unit 800, Toronto, ON, Canada,
M4W 3P4
golden@esit.com

Pinhas Ben–Tzvi [b]
[b] University of Toronto
Robotics and Automation Laboratory
Department of Mechanical and Industrial Engineering
5 King's College Rd., Toronto, ON, Canada M5S 3G8
pinhas.bentzvi@utoronto.ca

Commercially there are well established technologies of locomotion for mobile robots. Most of these technologies have been developed for urban (see structured) terrain, including climbing and descending of stairs and of various obstacles. In parallel, a number of technologies have been developed in laboratories, but have not reached the commercial market. There is a lack of new technology on the market, and serious problems arise as a result (IP infringement). We are identifying some of the reasons for lack of novel mechanisms for mobility in the commercial market. This issue is reflected also in other domains of robotics. Ways to mitigate the problem are presented. Two new technologies of mobility over unstructured terrain are introduced. The developments have been embodied in demonstration and commercial prototypes.

I. INTRODUCTION

Two decades ago, most mobile robots were slow–moving research platforms rolling through university corridors. Nowadays, mobile robots are starting to explore various outdoor environments for a variety of application domains, such as military, police and hazardous site exploration, surveillance, and reconnaissance. However, as the convenience of a laboratory is left behind, development, debugging, testing, and end-user operations are becoming more difficult. While in the laboratory, many mobile robot developers use tethers to link the onboard computer to a convenient desktop monitor and keyboard. Away from the lab, notebook computers on the robot are often used to give commands and to develop or modify software.

The transition from "structured" to "unstructured" environments is the greatest challenge in the field since the physical interaction of the robot with the environment is in general very complex and strongly influences the overall system's performance. Thus, the introduction of robots to unstructured terrain has required fundamentally different approaches to mobility in response to interaction with the environment.

There are numerous designs of mobile robots for unstructured environments such as PackBot[1], Remotec-Andros robots [2], Wheelbarrow MK8[3], AZIMUT[4], LMA[5], Matilda[6], MURV-100[7], Helios robots[8-9], Variable configuration VCTV[10], Ratler[11], MR-5 and MR-7[12], NUGV[13], and Talon by Foster Miller[14]. Mobile robot designs are mainly based on wheel mechanisms, track mechanisms and a combination of both.

Increasingly, mobile robotic platforms are being proposed and used in rough terrain and high-risk missions for law enforcement and military applications (e.g., Iraq for IED – Improvised Explosive Devices, detection), hazardous site clean-ups, and planetary explorations (e.g., Mars Rover). These missions require the mobile robots to perform difficult locomotion and dexterous manipulation tasks.

Various robot designs with active control of traction[1,2], sometimes called "articulated tracks", were found to improve rough-terrain mobility because of their capability to reposition the mobile robot center of gravity (COG). The repositioning of COG allows certain degree of control over the robot stability over uneven terrain. In this paper we present new technologies for enhanced mobility over unstructured terrain.

A new technology of mobile robot design (LMA[5]) is presented. It allows better control of COG location thus generating higher robustness to terrain unevenness. This was achieved by designing the robot with a variable track configuration using a pair of planetary arms.

Another aspect of novelty in this paper is a new design paradigm of mobile robots for locomotion and manipulation purposes. Typically, a mobile robot's structure consist of a mobile platform that is propelled with the aid of a pair of tracks, wheels or legs, and a manipulator arm attached on top of the mobile platform to provide the required manipulation capability (of hazardous materials, neutralization of bombs, etc). There are several designs of mobile robots that have pushed further the state of the art, such as PackBot[1] and Chaos[15], to include the ability to return itself when flipped-over. However, this may not be possible if the robot is equipped with a manipulator arm. This issue is addressed by the new design paradigm that provides locomotion and manipulation simultaneously and interchangeably.

II. IDENTIFICATION OF RESEARCH PROBLEMS AND APPROACHES

A detailed literature review and discussions with users has assisted us in identifying major issues of design of mobile robots used in field operations. These issues lead to new design problems and approaches to solutions. They are

briefly defined below:

1) Issue: In current designs the platform and manipulator arm are two separate modules that are attachable to and detachable from each other. The platform and the arm have distinct functions that cannot be interchanged.

Design problem: Each module contributes separately to design complexity, weight, and cost.

Approach to solution: The manipulator arm and the mobile platform are designed and packaged as one entity rather than two separate modules. Yet, the modules are attachable and detachable. The mobile platform is part of the manipulator arm, and the arm is part of the mobility platform. Fewer components are required, and this may result in a simpler and more robust design, weight reduction and lower production cost.

2) Issue: In all mobile robots that include a manipulator arm, it is always mounted on top.

Design problem: The arm is exposed to the surroundings, and is susceptible to breakage and damage especially when a flip-over occurs.

Approach to solution: The arm and platform are designed as one entity, and the arm is nestled in the platform. This eliminates the exposure of the arm to the surroundings while the platform is moving in particular in close or narrow areas (e.g. an underground tunnel). As soon as the target is reached, the arm is deployed to execute desired tasks.

3) Issue: Better mobility is achieved without a manipulator arm.

Design problem: Without an arm the functionality is limited as it cannot provide manipulation capability.

Approach to solution: The arm and platform are designed as one entity, and the arm is nestled in the platform. Since the arm is part of the platform, it is not exposed to the surroundings, and mobility is enhanced.

4) Issue: When operating over unstructured terrains, robots may reach positions from where they could not be righted /controlled further for a purpose. Some designs provide various active means of self-righting.

Design problem: To provide self-righting without special purpose or active means.

Approach to solution: The platform is fully *symmetric* even with the manipulator arm mounted on, thus allowing the robot to continue to the target with no need of self-righting when it flips over.
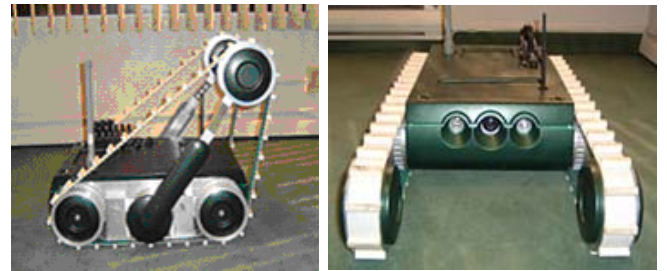
The above approaches have common denominators: they are focused on robot functionality, and they can be realized by a global approach. This approach is the new design paradigm presented in the paper.

III. LMA - LINKAGE MECHANISM ACTUATOR

III.A. Mechanical Structure of LMA

Views of LMA are shown in Fig. 1. The mobile robot has two pairs of fixed wheels at the front and rear of the chassis. Two arms are installed on both flanks of the frame, and two wheels are attached at their tip via a spring loaded prismatic joint to retain tension in each track. The arms are parallel, and are rotated together by one motor. The set of two arms is called "flipper". By rotating the flipper, the track configuration changes facilitating greatly the climbing of obstacles, including climbing and descending stairs and slopes. The flipper rotation is constrained by a cam mechanism that generates an elliptical path of the tip of the flipper arm. The platform is symmetric with respect to front and back sides. Each track is rotated by a motor independently, so that LMA can not only go forward and backward, but also turn left, right and around. An anchor is also available on the frame to install an optional robotic arm. As a case study, autonomous stair climbing with the LMA is presented in order to demonstrate the advantageous mobility characteristics of this new platform.

<div align="center">(a) Side view   (b) Front view</div>

Fig. 1 Side and front views of the LMA

III.A.1. Relationship of Flipper Angle and Length

The relationship of the flipper angle with the longitudinal axis of the platform and its corresponding flipper length is given by equation (1). The parameters used in the calculation are defined in Fig. 2. The flipper angle is denoted by φ, and its value is zero degrees when the flipper is extended to the front (and 180 deg for the back). The flipper length, $l(\varphi)$ is the distance between the flipper tip and the flipper joint located at the center of the chassis. The longest and shortest lengths of the flipper due to its spring loaded prismatic joint are denoted as *a* and *b,* respectively. The shortest flipper length is when the flipper is perpendicular to the frame (i.e., $\varphi = \pm 90^o$), while the longest flipper length is when the flipper extends to the front or rear (i.e., $\varphi = 0^o$ or $\varphi = 180^o$).

$$l(\varphi) = \sqrt{\frac{a^2 b^2}{b^2 \cos^2 \varphi + a^2 \sin^2 \varphi}} \qquad (1)$$

Some specifications of the LMA are provided in Table 1.

TABLE I. General specification of the LMA

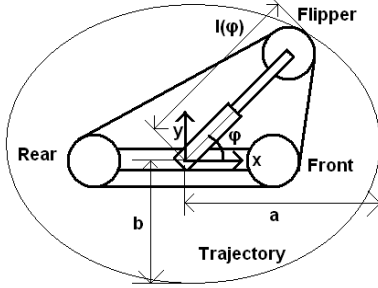| Name	Parameter	Dimension
Wheelbase	L	400 mm
Longest Flipper Length	a	466 mm
Shortest Flipper Length	b	421 mm
Wheel Radius	r	74 mm
Weight	w	25.0 kg

Fig. 2 Parameters for flipper length calculation

Of the three motors situated in the robot chassis, two motors are propelling the left and right tracks, and the third one is rotating the flipper. Encoders connected to the motors are utilized to establish closed-loop position, speed or acceleration control of the motors.

III.A.2. Sensors

The LMA is equipped with a thermometer, GPS, three-axis compass and battery-voltage monitor. The three-axis compass manufactured by Honeywell provides pitch, roll and yaw (heading direction) angle with a sampling frequency of 8Hz. The range of the heading direction is 360^0 and that of roll and pitch angles is $\pm 60^0$. The package is composed of single and two-axis magnetic sensors, as well as a two-axis accelerometer.

III.B. Automatic Stair Climbing Procedure

The schematic in Fig. 3 shows the stair profile used and some relevant parameters. The height of each step or riser length ranges from 12 to 18 cm and the width of a step ranges from 8 to 25 cm. The imaginary line connecting the stair edges is referred to as the 'nose line'. The slope of a nose line indicates how steep the stairs are; it ranges from 25 to 45^0. Stairs with step height and width of 18 cm and nose line slope of 45^0 were used to test LMA.
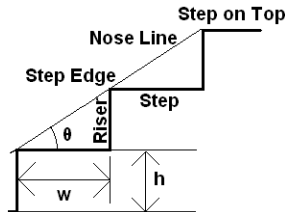

Fig. 3 Stair profile and parameters

The motion required to climb stairs is broken down into three stages: "moving to nose line", "riding on nose line" and "landing". Fig. 4 shows the complete procedure to climb stairs[16]. In the "moving to nose line" stage, LMA moves forward until its flipper wheels are above the first step edge as shown in Fig. 4(a) and (b). During this stage, the flipper is pre-set by the user at a certain angle (approx. 45^0), such that some of the treads on the tracks would hook onto the first step edge, and the robot will start climbing as shown in Fig. 4(c). Then, the flipper is rotated backwards until its tip touches the ground and the COG has crossed over the edge of the first step, and is now positioned over the step (Fig. 4(d)). While the LMA moves forward (Fig. 4(e)), the flipper continues to rotate in same direction until is fully extended along the longitudinal axis of the LMA. Then the flipper is stopped, and the LMA is 'riding on nose line' as shown in Fig. 4(f). During the 'riding on nose line' stage, the heading direction needs to be adjusted, for example in case of uneven, curved or spiral stairs.

LMA maintains this stage until the leading wheels are suspended above the step at the top. The purpose of the 'landing' stage is to prevent the robot from a free fall over the step at the top. In order to do so, the flipper is slightly rotated downwards as shown in Fig. 4(g), while LMA moves forward. When the COG has crossed the top step edge and it is over the step, the flipper reverses its rotation until it is fully extended to the rear (Fig. 4(h)), while the LMA continues to move forward. In cases where "hard landing" is acceptable, it may not be required for operators to follow the landing procedure, and it can be skipped during the autonomous climbing procedure. The procedure for descending stairs is accomplished by a reverse sequence of stages required to climb the stairs (Fig. 4). In this case, the robot may descend from its rear end, with no need to rotate in order to descend with the same leading wheel as during the climbing.

III.C. Stability Analysis for Climbing Stairs

For reliable autonomous climbing of stairs stability judgment equations were formulated for real-time monitoring to assess the risk of flipping over. By calculating inclination thresholds that may result in unstable positions and adding certain margins to them, LMA was successfully stopped before it was in danger of tipping or falling off. The equations and algorithms for some of the cases are shown below.

III.C.1. Stability Judgment Equations

The mathematical relationship between the flipper angle φ and LMA inclination θ is derived for illustration with respect to some specific configurations as follows: (i) LMA with flipper suspended; (ii) with flipper at rear; and (iii) LMA on nose line.
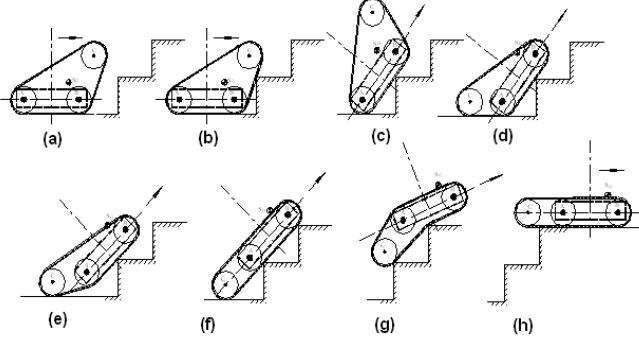
Fig. 4 Climbing and descending procedures for stairs
Climbing follows the order of (a), (b), (c), (d), (e), (f), (g), (h)
Descending follows the order of (h), (g), (f), (e), (d), (c), (b), (a)

(i) LMA – Flipper Suspended

The configuration to be considered is depicted in Fig. 5(a), showing the leading wheels on the first step edge and the flipper in the air. A Cartesian coordinate frame is aligned with the origin located at the center of the rear wheels and its x axis parallel with the robot's frame. On this coordinate frame, the location of center of gravity of LMA (COG in Fig. 5) is expressed as G_x and G_y with respect to x and y axis, respectively.

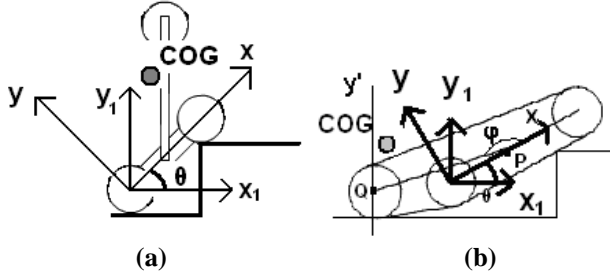**(a)**   **(b)**

Fig. 5 (a) LMA with Front wheels on step edge; (b) LMA with flipper wheels at the rear

The coordinate of the COG on x_1 axis is given by:

$$G_{x1} = G_x \cos\theta - G_Y \sin\theta \qquad (2)$$

where θ is the robot inclination that is measured by the 3-axis compass. To avoid flipping over from the first step on the stairs, the COG must be maintained on the right side of y_1 axis. Therefore, condition $G_{x1} > 0$ must be satisfied. Substituting this condition into equation (2) and solving for G_x yields the following stability judgment equation:

$$G_x > G_y \tan\theta \qquad (3)$$

(ii) LMA – Flipper at Rear

In the configuration shown in Fig. 5(b), LMA chassis has inclination θ, flipper angle φ (between 90 and 270^0), and the tip of the flipper sustains LMA on the ground. To avoid flipping over of the robot, the COG must be maintained at the right side of y' axis as indicated in Fig.

5(b). Therefore condition $G_{x1} > Q_{x1}$ must be satisfied. Solution of this condition for G_x yields the following stability judgment equation:

$$G_x > G_y \tan\theta + \frac{L}{2} + l(\varphi)\frac{\cos(\theta+\varphi)}{\cos\theta} \qquad (4)$$

(iii) LMA on Nose Line

The required conditions for a mobile robot on a nose line have been documented [17]: (i) half of the wheelbase of a mobile robot is larger than the distance between two adjacent step edges; and (ii) mobile robot's COG is over the step edge which the robot engages rearward. With these conditions the following conditions were derived:

$$\theta \geq \sin^{-1}\frac{2h}{L/2+l(180°)-r} \qquad (5)$$

$$G_x > \frac{L}{2} - l(180°) + \frac{h}{\sin\theta} + (G_y + r)\tan\theta \qquad (6)$$

III.D. Range of COG Coordinates

The position of the robot's COG is a function of the flipper angle. One of the methods to obtain the COG coordinates is to perform real-time calculations. This is undesirable as it significantly adds to the computational load. To avoid this real time task, the range of the LMA COG was identified. In order to find the range, the relationship between the robot's COG position and its flipper angle was derived. With the derived equations we identified the maximum ($G_{x,\max}$) and minimum ($G_{x,\min}$) of the COG on the x coordinate (φ is 0 and 180^0, respectively) and the maximum ($G_{y,\max}$) and minimum ($G_{y,\min}$) of the COG on the y coordinate (φ is 90 and 270^0, respectively).

The LMA's COG is in the range defined by the four values above. Therefore, with those constant values, a real-time computation of COG position can be avoided and equations (3), (4), (6) are replaced by the following conditions, respectively:

$$G_{x\min} > G_{y\max} \tan\theta \qquad (7)$$

$$G_{x\min} > G_{y\max} \tan\theta + \frac{L}{2} + l(\varphi)\frac{\cos(\theta+\varphi)}{\cos\theta} \qquad (8)$$

$$G_{x\min} > \frac{L}{2} - l(180°) + \frac{h}{\sin\theta} + (G_{y\max} + r)\tan\theta \qquad (9)$$

III.E. Algorithms for Stability Judgments

During autonomous climbing of stairs, some tasks are running concurrently. They include: sending requests to the compass, receiving frames from the sensor and the remote controller and judging stability, and executing autonomous climbing procedures. In this section, the algorithms related to stability judgment equations are developed.

The stability judgment equations corresponding to the robot's configuration are continuously evaluated based on up-to-date robot's inclination measurements, while the robot is moving. If any of the equations are violated, the robot performs a certain behavior as follows.

If equation (7) or (8) is not satisfied, LMA stops right away, and autonomous climbing terminates. This algorithm is named stability judgment thread 1 (abbreviated as S.J.T 1). The corresponding flowchart is shown in Fig. 6(a).

In the case that equations (5) or/and (9) are violated, LMA stops right away and waits three seconds followed by another evaluation of both equations. Nevertheless, if both or either equation is/are still not satisfied, autonomous climbing is terminated; otherwise, LMA resumes motion. The algorithm is called stability judgment thread 2 (abbreviated as S.J.T.2), and is summarized in a flowchart shown in Fig. 6(b). This algorithm to stop LMA was incorporated to overcome the effects of noise associated with inclination data measurements while LMA is climbing stairs on a nose line.
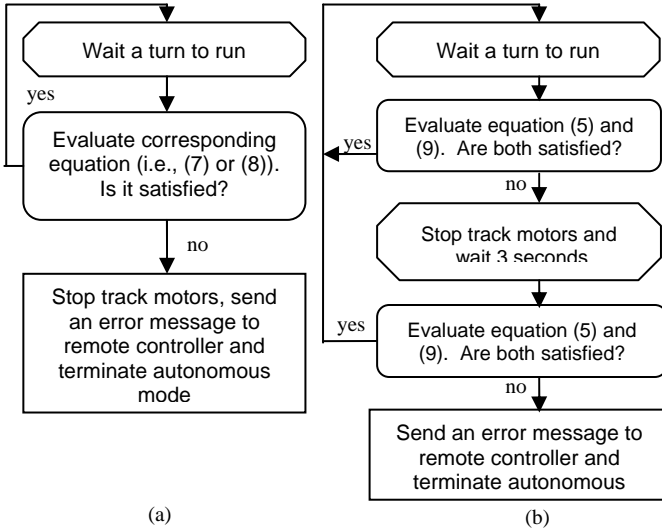

(a)   (b)

Fig. 6 (a) Stability judgment thread 1; (b) Stability judgment thread 2

III.F. Algorithms for Autonomous Climbing of Stairs

During autonomous climbing, LMA depends on measurements from its inclinometer (the 3-axis compass) and the encoders attached to the three motors. By interacting with those sensors, autonomous climbing is performed based on climbing procedures mentioned earlier. The algorithms to autonomously climb stairs are divided into four stages: measuring step height, moving to nose line, riding on nose line, and landing. Furthermore, the stability judgments equations derived in Section III.C are incorporated in the algorithms as well. In this section we select for discussion the algorithm related to riding on nose line.

Climbing Task Stage 3: Riding on Nose line

The LMA moves forward on the nose line and the slope of the nose line is continuously measured. The required motions to accomplish this stage are summarized in the flowchart shown in Fig. 7.
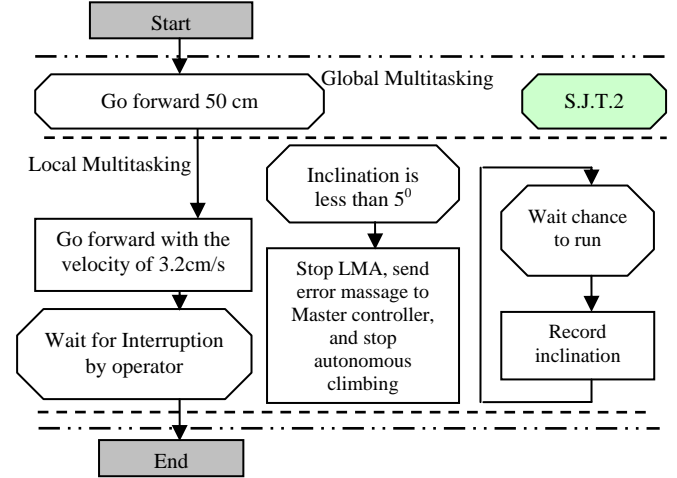

Fig. 7 Flowchart of riding on nose line stage

III.G. Experimental Setup and Results

The implementation and validation of autonomous climbing presented some problems. They are discussed in this section.

III.G.1. Signal Analysis and Filters

The signal from the compass had excessive noise while the robot was moving. The signal was analyzed and algorithms and filters were designed to remove noise effects.

Signal Analysis

Fig. 8 shows raw inclinations signal from the 3-axis compass while LMA was riding on the nose line as shown in Fig. 9(c). When LMA is on the nose line, the inclination is supposed to provide readings of the slope (i.e., 45^0). However, we observed that the signal was very noisy. The main factors are: (1) slips between treads and step edges; and (2) oscillation of the chassis.

$4 - 7$ Hz noise is caused by LMA's frame oscillation while riding on the nose line. This occurs because the segment of the tracks between the flipper wheels and the rear wheels bends when the stair edge touches that area (Fig. 9(a)). Therefore, the compass shows a slightly larger value than the actual slope of the nose line. In cases when the step edges are positioned under the wheels as shown in Fig. 9(b), the inclination measured by the compass coincides with the actual slope of the nose line.
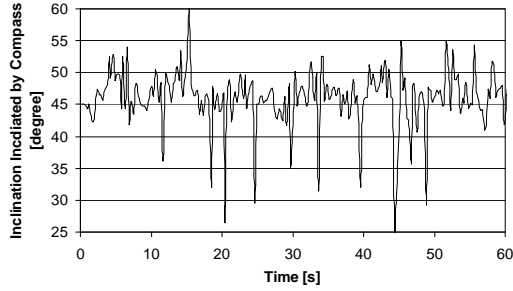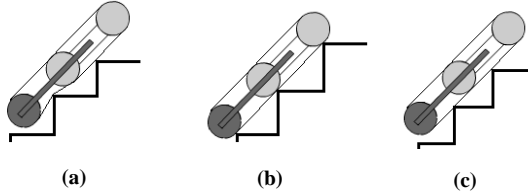
Fig. 8 Raw data from compass

Fig. 9 Inclination changes with the position of the LMA

III.G.2. Noise Elimination

Two serially connected filters were designed in order to remove the noise from the measured inclination signal to guarantee stable autonomous climbing.

Filter 1: Algorithm for Pulse Elimination

With this filter the abrupt pulses created by slip occurring between the treads and step edges were removed. In this algorithm, if the difference between new inclination data from the compass and the previous value is five degrees or more, the output of Filter 1 holds the same value; otherwise, the new value is output. This means that the data points from the compass are blocked until they settle within a certain range, thereby eliminating pulses having a magnitude of 5^0 or greater.

Filter 2: Digital Filter

The second filter is a low-pass digital filter used to remove noise caused by the oscillation of the chassis and other miscellaneous factors such as effects caused by electronic devices. The deviations created by LMA positions on a nose line are not considered noise, but rather real inclination changes that might cause LMA to flip over in some cases. Therefore, Filter 2 would pass those deviations. By considering their highest calculated frequency (0.137 Hz), the filter cut off frequency ($\mathbf{f_c}$) was set at 0.20 Hz. The frequency response of this filter confirmed that the filter is low-pass.

The two filters designed above were connected in series resulting in high frequency components being cut off after impulses are eliminated. With this set of filters, the raw data shown in Fig. 8 become the signal shown in Fig. 10. The output deviations from the slope of the nose line are restricted within seven degrees.
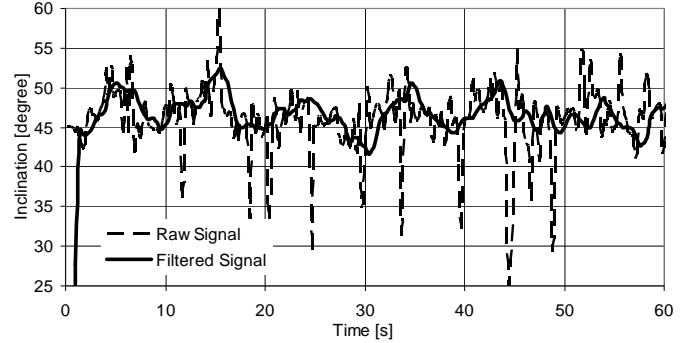

Fig. 10 Effect of Filters 1 and 2 connected in series

IV. HYBRID MOBILE ROBOT – HMR

In response to the issues addressed in Section II, this section introduces a new mechanical design paradigm for mobile robot and manipulator system.

The new approach is based on hybridization of the mobile platform and manipulator arm as one entity for robot locomotion as well as manipulation. The approach is that the platform and manipulator are interchangeable in their roles in the sense that both can support locomotion *and* manipulation in several configuration modes. Such a robot can adapt to various ground conditions better than the state-of-the-art.

The proposed idea is two-fold as follows:
(i) The manipulator and the mobile platform are integrated as one entity to yield a hybrid mechanism rather than two separate and attachable modules. Consequently, the some of the joints (motors) that provide manipulator's dof's also provide mobile platform's dof's;
(ii) Robot's mobility is enhanced such that when a flip-over occurs, instead of trying to prevent the robot from flipping-over or attempting to return it, the platform will be "allowed" to flip-over and continue to operate.

IV.A. Description of the Concept

The embodiment of the proposed idea is depicted in Fig. 11. If the platform is inverted due to flip-over, the fully *symmetric* nature of the design (Fig. 11(a)) allows the platform to continue to the destination from its new position with no need of active means of self-righting. Also it is able to deploy/stow the manipulator arm from either side of the platform.

The platform includes a couple identical and parallel base link 1 (left and right), link 2, link 3, wheel tracks, end-effector and passive wheel(s). To support the symmetric nature of the design, all the links are nested into each other. Link 2 is connected between the base link tracks via joint 1 (Fig. 11(b)). Two wheel tracks are inserted between links 2 and 3 and connected via joint 2, and a passive wheel is
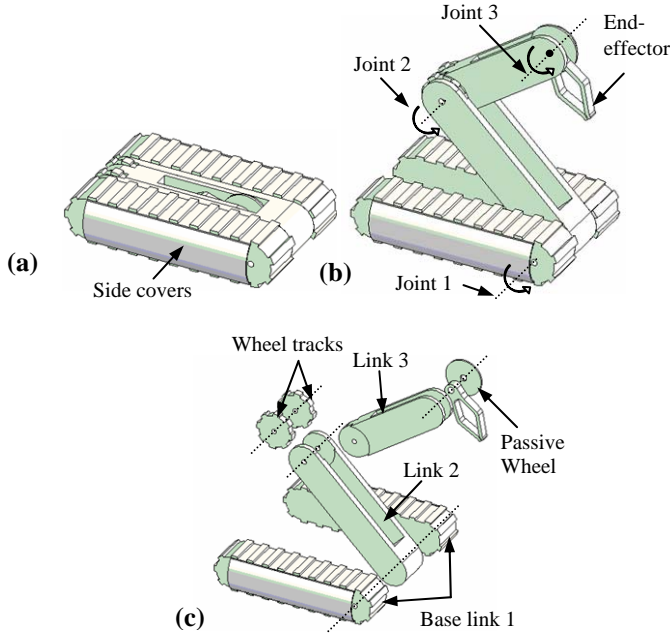
6

Fig. 11 (a) closed configuration; (b) open configuration; (c) exploded view

inserted between link 3 and the end-effector via joint 3 (Fig. 11(c)). The wheel tracks and passive wheels are used to support links 2 and 3 when used for various configuration modes of traction. Link 2, link 3 and the end-effector are connected through revolute joints and are able to provide continuous 360° rotation and can be deployed separately or together from either side of the platform. To prevent immobilization of the platform during a flip-over scenario, rounded and pliable covers are attached to the sides of the platform as shown in Fig. 11(a).

IV.A.1. Configuration Modes of Operation

The links can be used in three modes: (a) All links used for locomotion to provide added level of maneuverability and traction; (b) All links used for manipulation to perform various tasks; (c) Combination of modes (a) and (b). While some links are used for locomotion, the rest could be used for manipulation at the same time, thus the hybrid nature of the design.

IV.A.2. Maneuverability, Traction and Manipulation

Fig. 12(a) shows the use of link 2 to support the platform for enhanced mobility as well as climbing purposes. Link 2 also helps to prevent the robot from being immobilized due to high-centering, and also enables the robot to climb taller objects (Fig. 12(b)). Link 2 is also used to support the entire platform when moving in a tripod configuration while using the other links for manipulation (Fig. 12(c)). For enhanced traction, the articulated nature of

the mobile platform allows it to be adaptable to different terrain shapes and ground conditions (Fig. 12(e)). Fig. 12(c) and (d) depict two of the different configurations for manipulation purposes. While some links are used for locomotion, others are used simultaneously for manipulation.
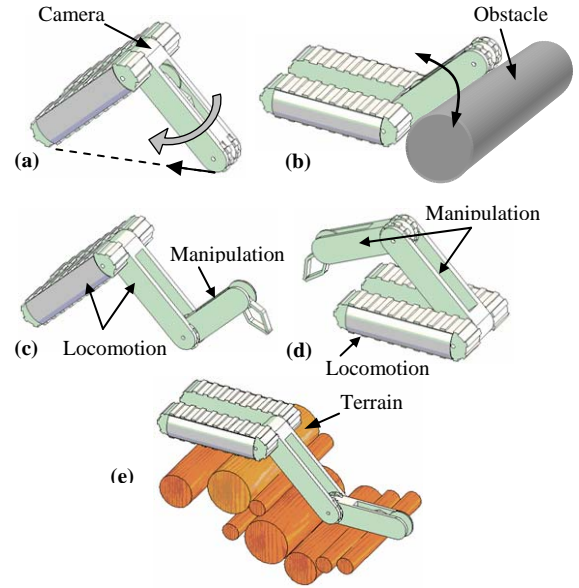

Fig. 12 (a),(b) sample mobility configurations; (c),(d) sample manipulation configurations; (e) configurations for enhanced traction

IV.B. Description of the Mechanical Design

The mechanical architecture of the mobile robot is shown in Fig. 13. Excluding the end effector, the design includes four motors (including gear-heads); two are situated at the back of each base link track to propel the tracks independently and the other two at the front to propel links 2 and 3 (Fig. 11).

The design also includes a built-in dual-operation track tension and suspension mechanism situated in each of the base link tracks. It includes spring suspended supporting planetary pulleys; three situated at the bottom of each track and another three at the top. While the bottom three supporting pulleys are in contact with the ground, they act as a suspension system. At the same time, the upper three supporting pulleys will provide a predetermined tension in the tracking system. The role of the pulleys at the bottom and top is interchangeable when the platform is inverted, thereby accounting for the symmetric design and operation of the mobile robot. Another usage of the spring array is to absorb some of the energy resulting from falling or flipping, thus providing compliance to impact forces.

A fully loaded depiction of the mobile manipulator is shown in Fig. 13. General specifications of the robot are provided in Table II.

7

IV.C. Modeling and Simulations of the HMR

Dynamic simulations of the complete robotic system

Table II. Robot Design Specifications

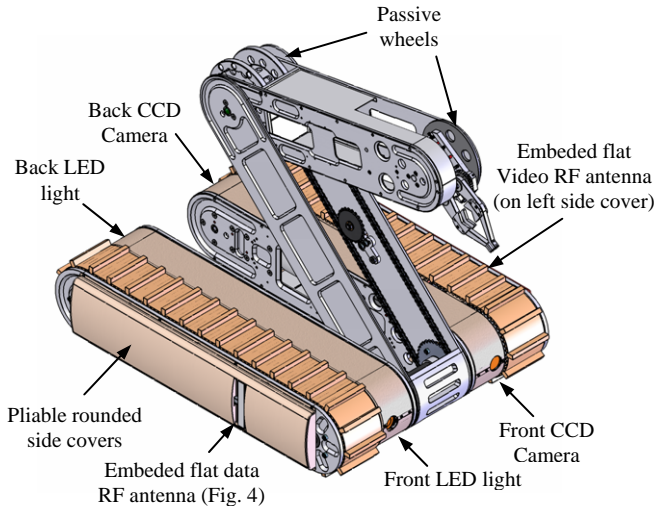| Total estimated weight (including batteries and electronics)	65 [Kg]
Length (arm stowed)	814 [mm]
Length (arm deployed)	2034[mm]
Width (with pliable side covers)	626 [mm]
Height (arm stowed)	179 [mm]

Fig. 13 Fully loaded HMR

were performed in order to study its functionality and optimize the design. The 3D mechanical design that was developed with the CAD Software was exported to ADAMS software[18] to perform simulations.

Simulations were performed for studying robot's functionality: various manipulation scenarios, flipping over due to a ramp obstacle, traversing pipes of different diameters, rectangular obstacle climbing and descending with different configurations, ditch crossing with different gap dimensions, stair climbing and descending, lifting tasks and more. A snap-shot is shown in Fig. 14.
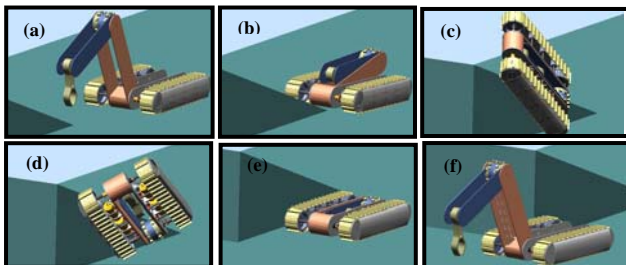

Fig. 14 Flip-over scenarios

V. CONCLUSIONS

We introduced two new technologies of mobility over unstructured terrain, LMA and HMR. The developments have been embodied in demonstration and commercial prototypes for the LMA. The developments presented were focused on mobility; however the second major component to the platform chassis, the arm, was also addressed with the Hybrid Mobile Robot. The HMR is being manufactured.

REFERENCES

1. T. Frost, C. Norman, S. Pratt, and B. Yamauchi, "Derived Performance Metrics and Measurements Compared to Field Experience for the PackBot", *In Proceedings of the 2002 PerMIS Workshop*, Gaithersburg, MD, USA (2002).
2. J.R White, T. Sunagawa, and T. Nakajima, "Hazardous-Duty Robots - Experiences and Needs", *Proc. IEEE/RSJ Int. Workshop on Intelligent Robots and Systems '89 (IROS '89)*, pp.262-267 (1989).
3. S. Costo, and R. Molfino, "A new robotic unit for onboard airplanes bomb disposal", *35th International Symposium on Robotics ISR 2004*, Paris, pp. 23-26 (2004).
4. F. Michaud, et al, "Co-Design of AZIMUT, A Multi-Modal Robotic Platform", *ASME 2003 Design Eng. Tech. Conferences and Computers and Info. in Eng. Conference*, Chicago, Illinois USA, Sep. 2-6, 2003, (2003).
5. A.A. Goldenberg, J. Lin, "Variable Configuration Articulated Tracked Vehicle", US Patent Application #11/196,486, Aug. 4, 2005.
6. S. Munkeby, D. Jones, G. Bugg, K. Smith, "Applications for the MATILDA Robotic Platform", *Proceedings of SPIE – Unmanned Ground Vehicle Technology IV*, Vol. 4715, pp. 206-213 (2002).
7. HDE Manufacturing, Inc., "MURV–100: The EOD, SWAT, and WMD Robot System," 2006. [Online]. Available: http://www.hdemfg.com
8. S. Hirose, E.F. Fukushima, R. Damoto, and H. Nakamoto, "Design of terrain adaptive versatile crawler vehicle HELIOS-VI", *Proc. IEEE/RSJ Int.Conf. on Intelligent Robots and Sys.*, Hawaii, pp. 1540-1545 (2001).
9. M. Guarnieri, P. Debenest, T. Inoh, E. Fukushima, S. Hirose, "Helios VII: a new vehicle for disaster response, mechanical design and basic experiments", Advanced Robotics, **19**(8), pp. 901-927 (2005).
10. T. Iwamoto and H. Yamamoto, "Mechanical design of variable configuration tracked vehicle", *Transactions of the ASME - Journal of Mechanical Design*, **112**, pp. 289-294 (1990).
11. J.W. Purvis, and P.R. Klarer, "RATLER: Robotic All Terrain Lunar Exploration Rover", *In Proc. Sixth Annual Space Operations, Applications and Research Symposium*, Johnson Space Center, Houston, TX., pp. 174-179 (1992).
12. MR-5 & MR-7 mobile robot. Available at www.esit.com, Nov. 2007.
13. M.R. Blackburn, R. Bailey, and B. Lytle, "Improved Mobility in a Multidegree-of-Freedom Unmanned Ground Vehicle (UGV)," *SPIE Proc. 5422: UGV Technology VI*, Orlando, FL, April 13-15, 2004.
14. TALON Mobile Robot, Foster-Miller. Available: http://www.foster-miller.com/lemming.htm, Nov. 2007.
15. P.J. Lewis, N. Flann, M.R. Torrie, E.A. Poulson, T. Petroff, G. Witus, "Chaos, an intelligent ultra-mobile SUGV: combining the mobility of wheels, tracks, and legs", *Proceedings of the SPIE–Unmanned Ground Vehicle Technology VII*, Vol. 5804, pp. 427-438 (2005).
16. S. Ito, "Autonomous Climbing and Descending of Stairs and Slopes by a Mobile Robot", M.S. Thesis, Univ. of Toronto, Canada (2007).
17. J. Lin, "Studies on Movement Conditions of Tracked Vehicles with Variable Configuration," Eng. Services Inc., internal report (2004).
18. S.M. Malik, J. Lin, and A.A. Goldenberg, "Virtual prototyping for conceptual design of a tracked mobile robot", *Canadian Conf. on Electrical and Computer Eng.*, Ottawa, Ontario, Canada (2006).